

# PROCESS CHAIN SIMULATION OF LASER CLADDING AND COLD METAL FORMING

P. KHAZAN\*, A. KZZO\*\*, R. HAMA-SALEH\*\*\*,  
A. WEISHEIT\*\*\*\*, I. ÜNSAL\*\*\*\*\* and M. BAMBACH\*\*\*\*\*

\**Simufact Engineering GmbH, 21079 Hamburg, Germany, pavel.khazan@simufact.de*

\*\**Simufact Engineering GmbH, 21079 Hamburg, Germany, abdullah.kzzo@simufact.de*

\*\*\**Fraunhofer-Institut fuer Lasertechnik, Steinbachstrasse 15, 52074 Aachen, Germany, rebar.hama-saleh@ilt.fraunhofer.de*

\*\*\*\**Fraunhofer-Institut fuer Lasertechnik, Steinbachstrasse 15, 52074 Aachen, Germany,  
andreas.weisheit@ilt.fraunhofer.de*

\*\*\*\*\**Chair of Mechanical Design and Manufacturing, BTU Cottbus-Senftenberg,  
Konrad-Wachsmann-Allee 17, 03046 Cottbus, Germany, uensal@b-tu.de*

\*\*\*\*\**Chair of Mechanical Design and Manufacturing, BTU Cottbus-Senftenberg,  
Konrad-Wachsmann-Allee 17, 03046 Cottbus, Germany, bambach@b-tu.de*

DOI 10.3217/978-3-85125-615-4-19

## ABSTRACT

Lightweight construction is still an important driver for innovations in production technologies. Recent developments in Laser Metal Deposition (LMD) and forming technology allow the production of lightweight sheet metal components with locally adapted properties, reducing the weight of parts. For example, using laser cladding, it is possible to reinforce critical areas of a sheet metal component, while other areas can still remain untouched and thus consume less material, reducing the overall weight of the component. Conventional production of such reinforced structures would require expensive and time-consuming machining steps. However, especially if it comes to sheet metal components that are to be mechanically formed, the induction of heat during laser cladding might lead to undesired properties of the final product due to distortion, residual stresses as well as changed material properties. Such effects can be investigated by means of structural welding simulation, but, if it comes to process chains, i.e. reinforced metal sheets that undergo forming processes, a process chain simulation covering forming and cladding steps is desirable. This approach would also answer the question of preferred process sequences. This article presents an approach for such a process chain simulation for a demonstrator made of aluminium EN AW 6016 undergoing one laser cladding and one cold forming process. The simulation considers the influence of the process sequence (forming-cladding vs. cladding-forming) and helps to select the proper process sequence as well as predicts properties of the final product.

Keywords: Laser cladding, cold forming, process chain simulation, sheet metals

## INTRODUCTION

Nowadays, lightweight design is one of the most important drivers for further developments in manufacturing technology. On the one hand, it allows the reduction of material usage, leading directly to overall reduction of material costs. On the other hand, lighter structures with structural properties that are comparable with conventionally built components lead to weight reduction of the final product, reduce the processing and

## Mathematical Modelling of Weld Phenomena 12

material costs and finally the efficiency of the product itself. A combination of cold forming and cladding processes can be useful to achieve such goals.

In this article we take a brief look at a common forming process, initially consisting of a single cold metal forming step. Usually, in mass production of complex features, sheet metal of constant thickness is used. This leads to increased material usage and weight as well as higher needed forces and decreased tools life cycle during forming. Alternatively, tailored blanks, especially patchwork blanks, can be used, which allow for a variable sheet thickness. Tailored welded and rolled blanks only allow for relatively simple thickness variation. With patchwork blanks more complicated designs are feasible, but the patches cannot be joined to the basic sheet metal yielding a full metallurgical bond. However, technologies like laser cladding [1] allow for flexible local adjustments of material thickness and thus structural properties. While challenges that arise from increased process complexity are to be addressed, the method clearly enables a reduced overall weight of a component. On the one hand, laser cladding, basically a surface welding process, might induce undesired residual stresses as well as change local material properties in an undesired way. On the other hand, one has to investigate which process chain direction is the most desirable one: a sheet of metal can be cladded and then formed or vice versa.

From the manufacturing point of view such investigations, especially concerning the question of the preferred process sequence, would need at least two sets of forming tools to be applied to undeformed wrought material as well to deformed but cladded material. At this point, numerical simulation of cladding and forming process is helpful to identify the optimal process sequence, also allowing the estimation of hidden target variables that are difficult or expensive to measure, like residual stresses, strains, and material state.

Processing of aluminium alloys by means of laser cladding has been described in the past [2] and is in general a common process nowadays. Calculation of such kind of properties is a relatively new field and – due to long process times – often needs some kind of model simplification and reduction [3]. However, in general such calculations are possible [4] and can, if detailed enough, also cover not only deformation effects but also evolution of residual stresses [5].

Incremental simulation of sheet metal forming processes is well-described [6] and is widely used in research and industrial applications. However, the coupling between a forming and a welding or cladding simulation might be challenging (due to possible different element formulations, strain decomposition approaches, different meshes and so on), but possible [7].

In the current investigation, a sheet made of aluminium grade EN AW 6016 undergoes local forming as well as local cladding. Finite element welding and forming simulation with data transfer in between the processes is applied in order to identify the desired process chain to achieve best possible component properties at the end.

### GEOMETRIES, MATERIALS AND EXPERIMENTAL SETUP

Laser cladding and forming of an aluminium sheet made of EN AW 6016 provided by Hydro Aluminium Rolled Products GmbH is investigated. Dimensions of the sheet are 80 mm x 80 mm x 1 mm. A drilled hole with a radius of 2.5 mm is positioned at the centre of the sheet, see fig. 1, left.

# Mathematical Modelling of Weld Phenomena 12

The mechanical properties of EN AW 6016 T4 are shown in Table 1.

**Table 1** Mechanical properties of EN AW 6016 T4

$R_{p0.2}$	$R_m$	$A_{80}$
90-130 MPa	>190 MPa	> 24%

## LASER CLADDING PROCESS

In the vicinity of the hole, a ring-shaped cladding with a radius of 10 mm is welded onto the sheet using powder material made of the same alloy as the base material (fig. 1, right). During cladding, the component is clamped on a copper plate with internal meandering cooling channels. Water is used as cooling liquid with an entrance temperature of 16°C. A flow of 6 l/min is maintained. The component is fixed on the cooling plate using a steel clamping device with an opening at the centre (fig. 2). This opening can have different shapes, depending on the area that has to be cladded. It is important to clamp an area as big as possible to ensure that the warpage of the sheet metal during the cladding process is minimized. The cooling plate and the clamping device are bolted together.

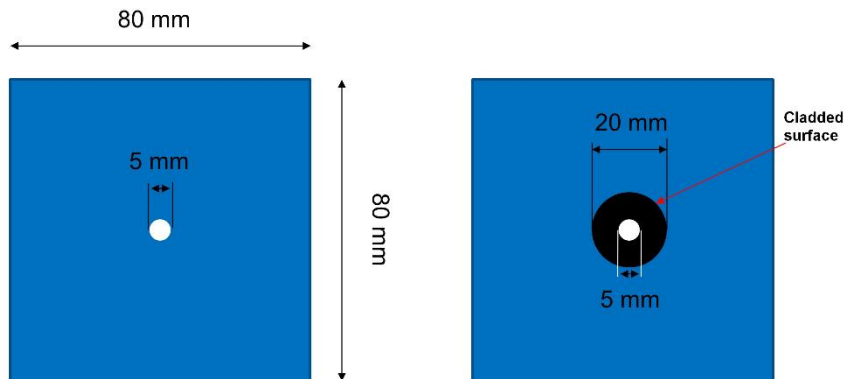


**Fig. 1** Left: Geometry of the aluminium sheet, right: cladded area.

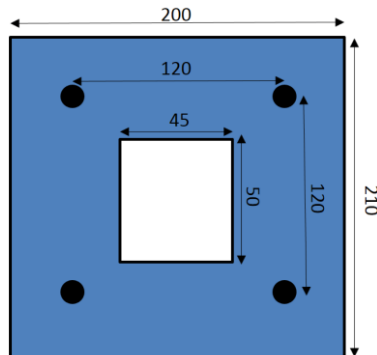


**Fig. 2** Geometry of the clamping tool.

## Mathematical Modelling of Weld Phenomena 12

Laser cladding is performed using a 2 kW Laserline LDF-2000 – 30 diode laser with the wavelength of 1030 nm. In a parameter study suitable process parameters were identified. To clad a thin sheet the local heat input must be minimized to avoid massive melting and warpage. Thus a laser spot diameter on the surface of 0.85 mm was selected for the process and the velocity is set to 4000 mm/min. The laser power required to clad a dense and bonded layer is 1200 W. A Laserline optic and an ILT powder feed nozzle are used. The powder is fed in an inert gas stream (Ar) with a GTV Twin powder feeder system into the interaction zone. To prevent oxidation of the melt pool the process zone is additionally protected by a local shielding gas stream (Ar) through the beam path opening. The complete experimental setup is shown in fig. 3. The cladding path itself is represented by an Archimedean spiral starting the edge of the hole and moving outwards. The distance between cladding tracks is approx. 0.3 mm while approx. 23 revolutions are required to achieve the outer diameter of 20 mm of the cladded area. With these settings, a cladding height of 0.25 mm in one layer was achieved. All this data was taken as input for the cladding model.

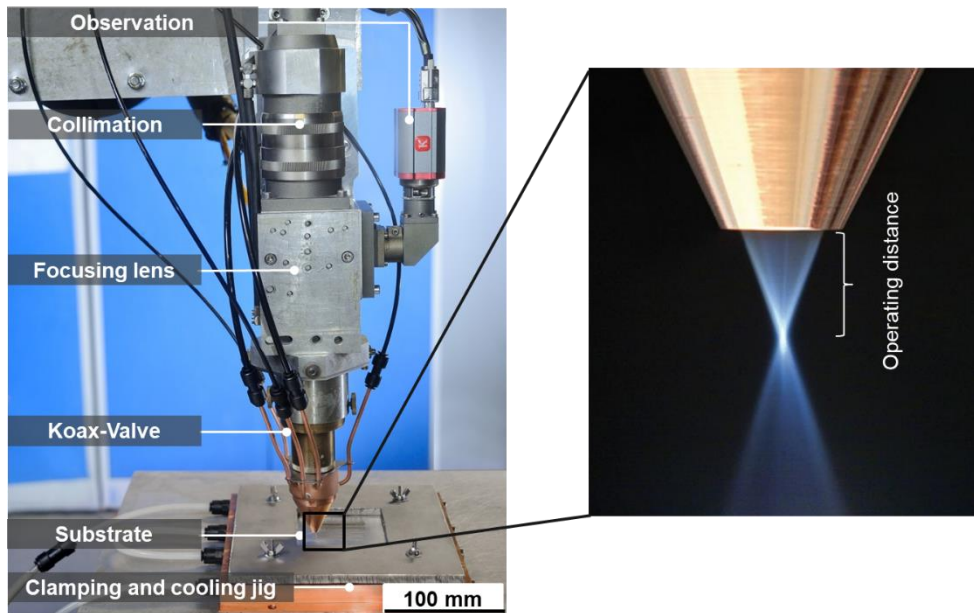


**Fig. 3:** Experimental setup for the laser cladding process with substrate, clamping and cooling-jig.

### FORMING PROCESS

The hole flanging experiments are executed on a Zwick Z250 universal testing machine. The machine can generate a testing force of max. 250 kN, which can be applied using a constant velocity for the forming tool. Additionally, the force used in the forming process can be measured continuously.

## Mathematical Modelling of Weld Phenomena 12

A special tool was designed for the forming process. The aim is to clamp and fix the cladded specimen during the action of the forming die. This is achieved by bolting. Furthermore, different inserts can be used to operate with different hole diameters. Tool and die are depicted in fig. 4.

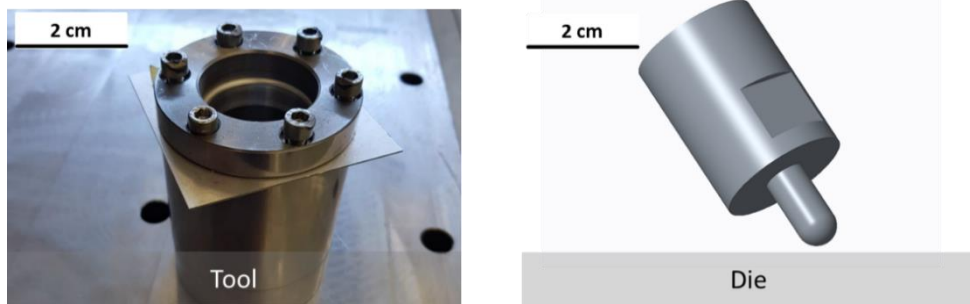
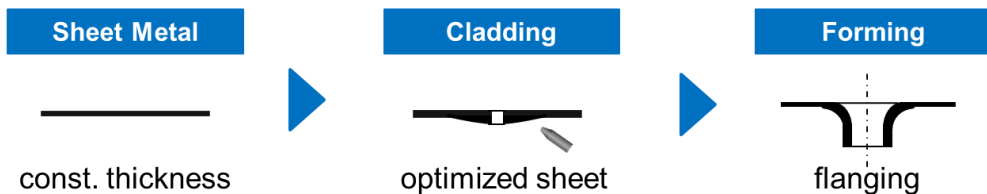


**Fig. 4:** Tool for collar forming (left) and CAD-Model of used die for forming process (right).

### *Forming of cladded sheet*

In this case, the hole flanging process is applied on a reinforced sheet metal. The die can be applied on the cladded and non-cladded side, leading to a different end geometry. It can be stated, that the flanging with the die on the cladded sides can lead to cracking of the cladded layer. The process chain is shown in fig. 5.

a)



b)

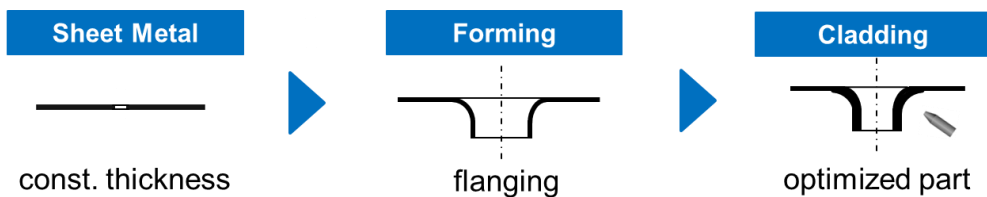


**Fig. 5:** Process chain for the sequence cladding-forming (a) and forming-cladding (b).

## FINITE ELEMENT MODELING

## Mathematical Modelling of Weld Phenomena 12

The welding as well as the forming processes were modelled using FE based software packages Simufact Welding and Simufact Forming, both in the most recent versions. The material model of aluminium EN AW 6016 was created using material simulation software JMatPro v. 9.1 by Sente Software. The material model respects dependences of thermal and mechanical properties on temperature. Additionally, stress-strain relations are described with respect to strain rate.

The fundamentals of FE-modelling of both – thermal and thermo-elasto-plastic – problems are well-described. Concerning heat transfer problems we refer to [8], while the fundamentals of plasticity can be found in [9] and the solution procedure by terms of finite element method is given in [10-11].

Both process chain directions – cladding and forming as well as forming and cladding – were calculated.

### PROCESS CHAIN CLADDING - FORMING

#### *Cladding model*

The cladding operation takes about 13.825 seconds with a total length of clad path of 921.6 mm. This is a relatively long clad line with relatively high cladding velocity, thus, the time discretization of the cladding process itself needs to be rather fine. In order to keep the calculation time sufficiently low, the main goal during model creation is the reduction of model complexity, thus, especially in the reduction of element number in the model.

The aluminium sheet was created from CAD data and meshed using Simufact Welding sheetmesher. The typical element edge length in the X-Y-plane of the sheet is between 0.13 and 0.33 mm in the cladding area and in the heat affected zone, while the general element edge length outside the relatively narrow heat affected zone is around 1.5 mm. Solid shell elements with seven layers are used for this component, reducing the number of needed element layers in the model to one. Through the usage of solid shell element approach the overall element number in this mesh can be reduced to 11,660, with approx. 23,700 nodes.

The cladding area (fillet mesh) is modelled as a disc with the height of 0.25 mm and radius of 10.85 mm using two layers of hexahedral elements with full integration and a typical element edge length of 0.125 mm, leading to 46,500 elements and 70,779 nodes within the cladding geometry. MSC Apex as well as Simufact Welding meshers were used for mesh generation.

In order to reduce the overall number of solid elements, the cooling plate is modelled as a rigid body using thermal properties of pure copper material. The temperature of the rigid body is set to 16 °C. The heat transfer between the cooling plate and the component is sufficiently high, governed by material properties of copper and aluminium assigned to the cooling device and the cladded component respectively. Such modelling approach creates an infinite heat sink.

The clamping device is also modelled as rigid body with usual 20 °C temperature. Both rigid bodies allow separation and sliding of the contacting surfaces, but no penetration. The general geometrical model is shown in fig. 6.

## Mathematical Modelling of Weld Phenomena 12

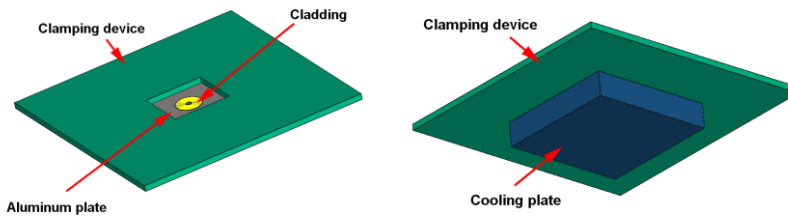


**Fig. 6:** Model geometry including base plate, cladded surface as well as cooling and clamping tools.

The cladding trajectory is directly imported from machine data; however, the number of sampling points has been reduced from over 9,000 to about 3,000. The equivalent heat source with an efficiency of 25% is positioned directly on the cladding, normal to the surface of the component, using a cylindrical shape with penetration depth of 0.4 mm and a radius of 0.42 mm. A constant clad flux distribution over the radius is assumed.

A fully adaptive time stepping scheme is used during the calculation. Initial and maximal allowed time steps are set to 2 ms and 5 ms, respectively, to allow for a good resolution of the process in terms of heat source movement. Convergence tests for the thermal solution are set to fulfil 20 K max. error in the temperature calculation as well as 1% max. tolerance in the force balance.

After the cladding process itself, the clamping tool as well as the cooling plate are both removed. This happens at 15 s and 20 s respectively. To avoid rigid body motion, at 20 s process time, nodal boundary conditions at three corners of the aluminium plate are activated, allowing free deformation but preventing any rigid body motion and rotation, thus being a classical three-point mounting support. The cooling duration is set to 1000 s; however, the calculation aborts after clamping tool and cooling plate removal as soon as the maximal temperature in all nodes of the model falls below 22 °C.

During the complete process, gravity, acting in the negative Z direction, is taken into account. Since solid shell elements in Simufact Welding and Forming solvers only support additive strain decomposition, this approach was also applied to solid elements present in the model.

### *Forming model*

Due to interoperability between Simufact Welding and Simufact Forming, the results of the cladding simulation can be easily transferred into a forming model. The mesh density of the welding model is also sufficient for the sheet metal forming simulation. The model geometry is rotated 180° around the centre point (so that the cladded surface showed in the negative Z direction) and is repositioned using contact and gravity positioners on the lower die. The movable upper die is attached to a press moving with velocity  $v = 44$  mm/min in the  $-Z$  direction until the stroke of 15 mm is achieved, thus leading to a deformation of the metal sheet including cladding. Both dies are modelled as rigid bodies without any deformations. Temperature effects are neglected. Fig. 7 shows the overall geometry of the model as well as die geometries in the contact area.

## Mathematical Modelling of Weld Phenomena 12

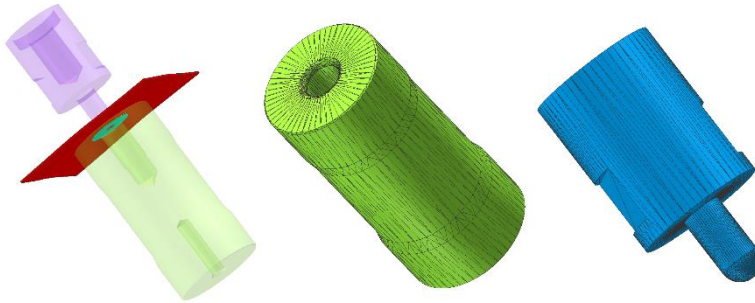


**Fig. 7** Forming model geometry (left), stationary die (centre), movable die/press (right).

After the desired stroke of 15 mm is achieved, the deep-drawing process stops, and the dies are removed. To avoid rigid body motion, stabilizer springs were added to the model.

### PROCESS CHAIN FORMING - CLADDING

#### *Forming model*

The model has the same configuration as the model used in the reversed process chain. In contrast to the cladding model in the cladding – forming chain, the cladding material is removed from the model and the dies were repositioned accordingly.

#### *Cladding model*

The-setup of the deformed sheet cladding model is significantly different from to the basic cladding model used in the previous process chain. Several challenges have to be solved in order to get useful model and results:

- The deformed sheet has to be repositioned on the cooling plate. This could be achieved using several positioning tools in Simufact Welding.
- The cladding geometry has to be created and positioned on the deformed shape. To achieve this, an expected shape of the contact area between base material and cladding material has been exported from the forming results. This contact surface has been meshed using 2D-shell elements, extruded normal to the surface and remeshed using the Simufact Welding mesher. Using gravity and contact positioner, the resulting geometry has been roughly pre-positioned on the deformed surface of the aluminium sheet. An intermediate solver run is then used to establish clean contact between component and cladding.
- Before welding, the assembly is clamped with the clamping tool, the four screws can apply a significant force and straighten the sheet. During the intermediate solver run this was achieved applying a certain force in the  $-Z$  direction of the clamp.



## Mathematical Modelling of Weld Phenomena 12

- After the intermediate solver run, the position of the clamp, the shape and positions of clamped sheet as well as the shape and position of the cladding material can be extracted and used for the cladding model.
- At this point no real process existed for this direction of process chain, thus, the description of welding paths was not available. The helix-shaped path was thus replaced by a number of circular paths beginning on the top of the deformed sheet and reaching the end of expected cladding geometry. The paths were calculated to get the same overlap as in the case of an Archimedean spiral.

The overall cladding period increased significantly (13.8 s vs. 17.0 s) compared to cladding of the undeformed sheet because of increased area after deep drawing process. The same holds for the weld path lengths (921 mm vs. 1134 mm). Thus, the overall heat input into the model increased by approx. 23%.

### SIMULATION RESULTS

#### *Chain Cladding - Forming*

After welding, cooling and unclamping the expected bending of the plate towards the laser beam occurs. Due to the fact that the corners of the plate are referenced at zero in Z direction, the distortion is visible as negative Z displacement of the plate, while the corners stay at the initial position (fig. 8).

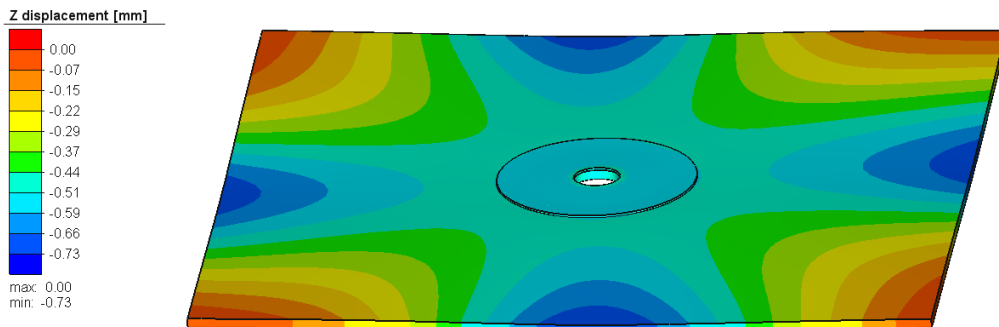


**Fig. 8:** Z-Distortion of the plate after unclamping, upper side.

On the lower side of the plate a sag is visible underneath the cladded surface, which can also be observed in the experiment (fig. 9). However, the absolute height is underestimated.

## Mathematical Modelling of Weld Phenomena 12

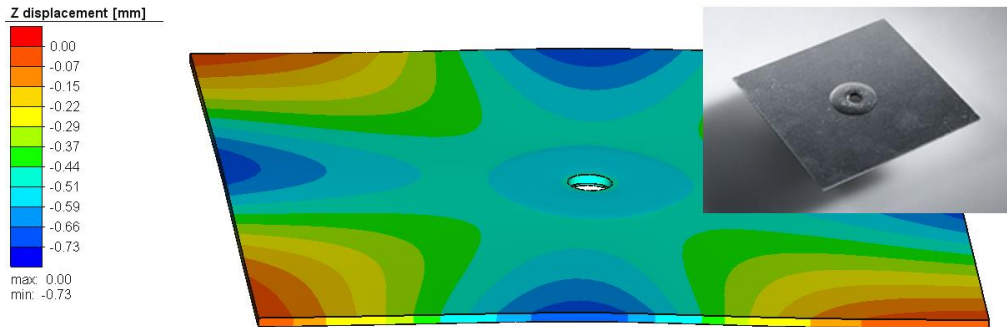


**Fig. 9:** Z-Distortion of the plate on the lower side (simulation and experiment).

The simulation also provides insight into residual stresses and the achieved yield stress during and after welding (fig. 10).

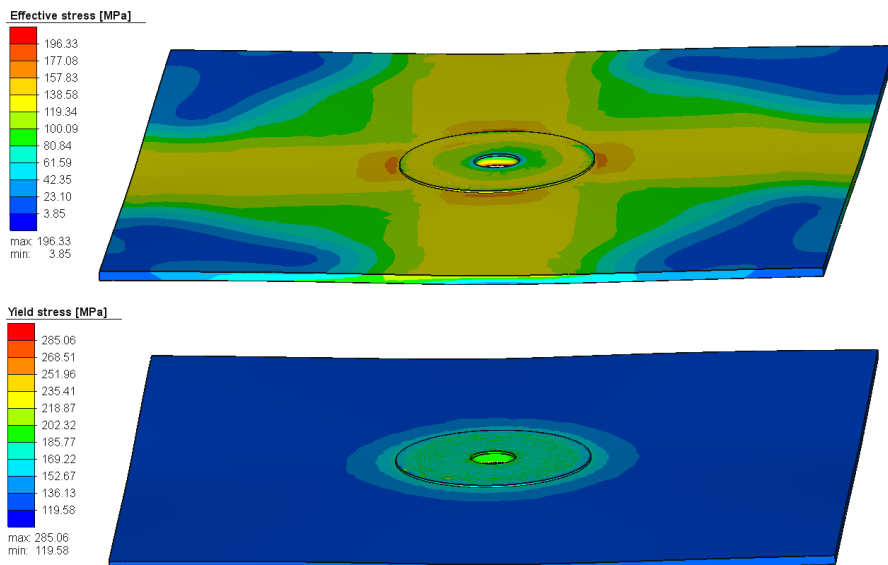


**Fig. 10:** Von Mises residual (top) and yield stresses after welding.

After forming and removing of dies, the deformation reaches 4.24 mm in the stroke direction at the centre of the plate. However, the plate itself is bent largely, showing 3.5 mm sag at the boundary of the plate (fig. 11).

## Mathematical Modelling of Weld Phenomena 12

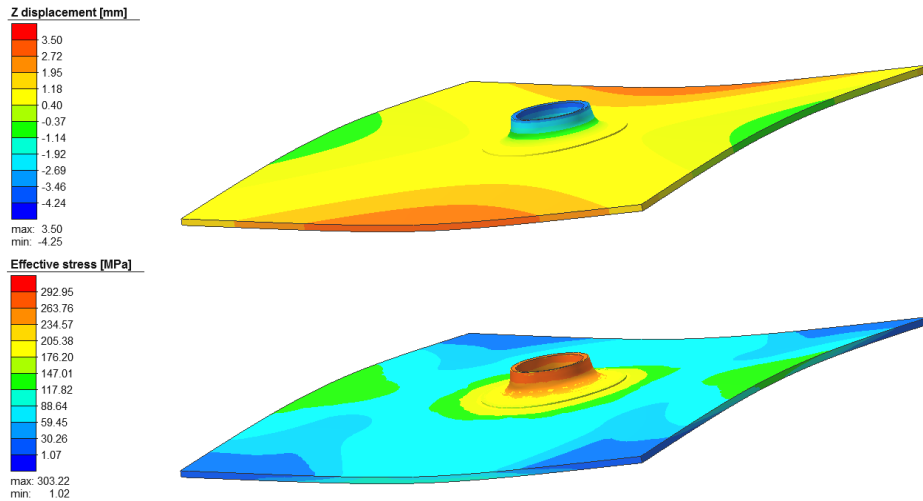


**Fig. 11:** Z-displacement (top) and von Mises residual stress (bottom) after forming.

In fig 11 high residual stress accumulation in the centre of the plate is also shown. In the cladding itself relatively high radial tensile stresses up to 400 MPa can be found in the base material directly in the contact area between base material and cladding.

The calculation time of this process chain using parallelization capabilities of Simufact FE-solver on a 16 core dual Intel® Xeon E5-2667 at 3.2 GHz machine was 27 hours for the cladding process and at about 2 hours for the forming process.

### *Chain Forming – Cladding*

The plate deformation after forming is nearly axially symmetric with respect to the Z-axis showing 4.4 mm Z-distortion in the stroke direction but less overall deformation of the plate reaching only about 1 mm at the edges of the plate (fig. 12). No significant additional distortion can be observed during welding. The von Mises stress after forming shows (at least in the area around the tools) similar peak values as before.

## Mathematical Modelling of Weld Phenomena 12

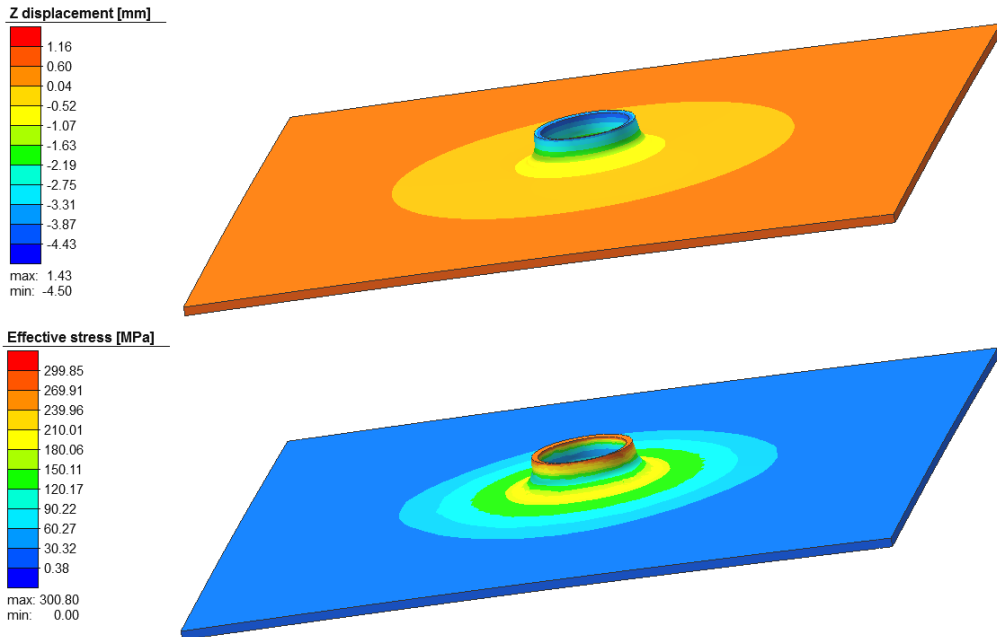


**Fig. 12:** Z-distortion (top) and von Mises residual stress (bottom) after forming.

After cladding, a reduction of residual stresses around the hole in the centre of the component (fig. 13) can be observed compared to uncladded, formed sheet.

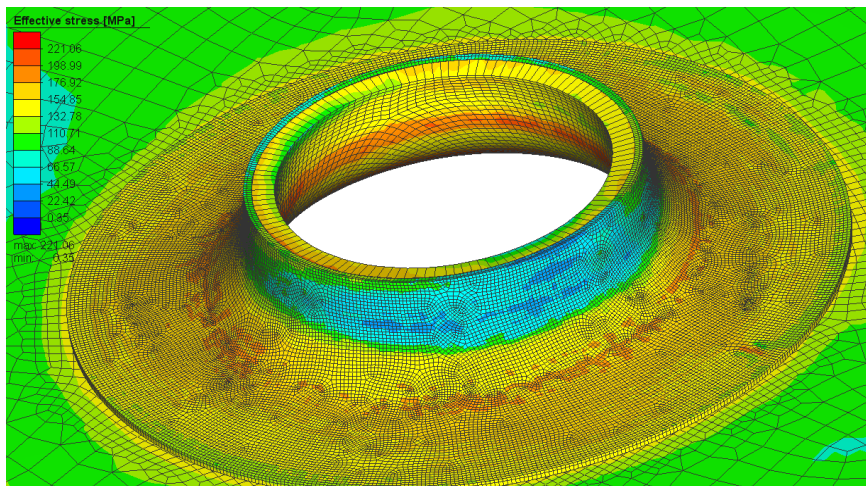


**Fig. 13:** Von Mises stress after forming, cladding, cooling and unclamping.

This can be explained due to the process chain direction, which leads to heating and partial melting of deformed material. Accumulated residual stresses and work hardening due to plastic deformations during forming are reduced. These reduced stresses also reduce the distortion, especially in the uncladded regions of the plate.

The calculation time of this process chain is approx. 0.6 h for the forming and 48 h for the cladding process.

## Mathematical Modelling of Weld Phenomena 12

### *Comparison of the two process chains*

Fig. 14 shows the deviation from the initial undeformed shape. Here, it is visible that the chain direction starting with forming leads to lower deformation of the initial geometry. The equivalent residual stress at the end of both process chains is widely different as shown in the figure 15.

Both effects are related, reduced residual stresses also reduce the deformation. Reduced residual stresses promise overall better characteristics of the component. Especially if the effective plastic deformation of the cladding is considered, the values achieved during the chain cladding  $\rightarrow$  forming are approx. three times higher compared to the reversed direction (fig. 16).

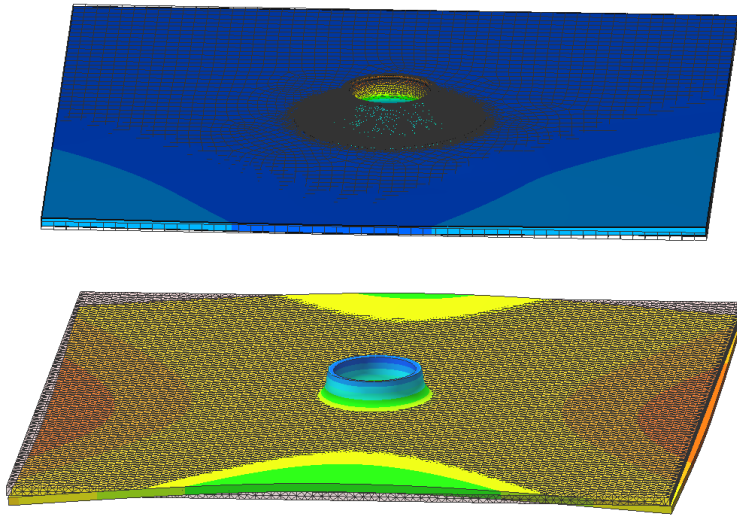


**Fig. 14:** Deviation from the undeformed state, top: forming  $\rightarrow$  cladding, bottom: cladding  $\rightarrow$  forming process chains. Solid: Simulation results. Wireframe: Initial shape.

## Mathematical Modelling of Weld Phenomena 12

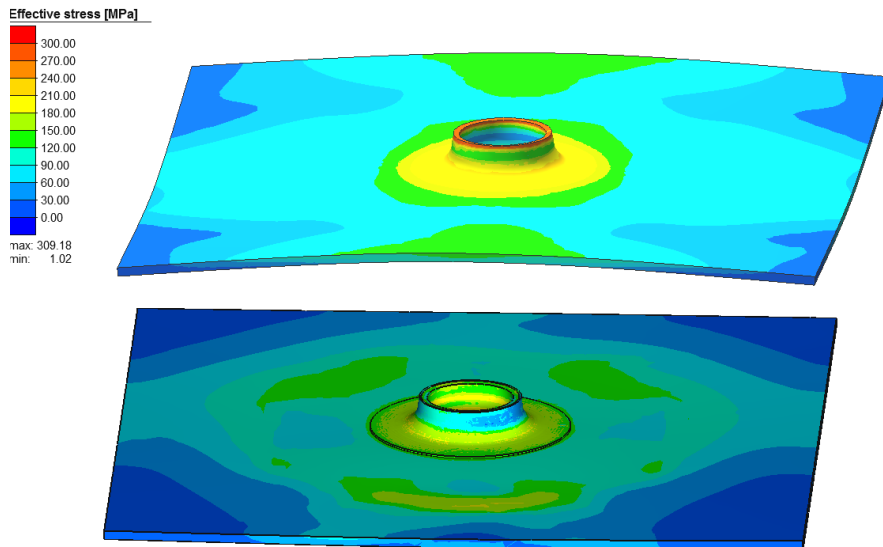


**Fig. 15:** Residual stress after cladding→forming (top) and forming→cladding (bottom) process chain.

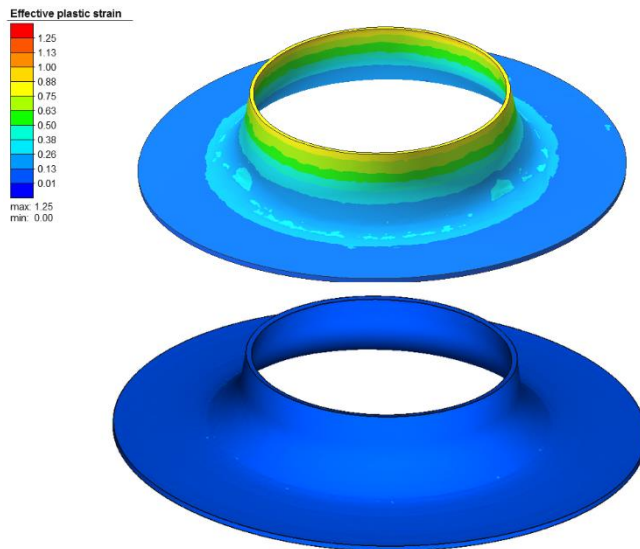


**Fig. 16:** Effective plastic strain at the end of the process, Cladding→Forming (top), forming→ cladding (bottom).

### CONCLUSION AND OUTLOOK

This work shows that it is possible to couple sheet metal forming and cladding process simulations if certain assumptions are met and if sufficient care is taken concerning correct plasticity formulation in both processes.

Besides already briefly discussed strain decomposition and element types, a proper material model that suits the needs of forming and welding simulation is needed. Such a material model can be obtained using material simulation software and adjusting the material properties according to measured data or material data sheets provided by manufacturer.

Due to partially missing experimental results it is difficult to make quantitative statements, however, qualitative conclusions can be made. Especially it is possible to select the best suited chain direction. The current investigation shows that cladding after forming seems to yield better results, i.e., less deviation of the underformed shape and lower residual stresses. For such a relatively simple model geometry this can be explained with two major effects. Firstly, deformations and residual stresses after forming are distributed nearly axial symmetric with respect to the Z-axis of the model. This leads to more balanced deformations and residual stresses after cladding. On the other hand, cladding process helps to relax forming residual stresses in the cladding area and also partially reduces the plastic strain and thus work hardening effects there. The reversed process chain suffers from asymmetrical residual stresses and deformations after cladding. Those imperfections are growing also during forming afterwards.

Future work will focus on validation of the models with experiments. Furthermore, a trimming stage between cladding and forming will be included. Investigations on the influence of tool geometry and hole diameter are planned, thus, the components are undergoing a cutting process after cladding and cooling, before the forming process starts. This might require remeshing and result mapping, while in the current work the same mesh could be used for all process steps.

The authors would like to thank BMWi (Federal Ministry for Economic Affairs and Energy) and AiF for funding of the IGF project 19292BG AiF/EFB “Lokale materialeffiziente Verstärkung belastungsangepasster Bauteile durch Laserauftragschweißen und Tape-Beschichten”.

The contribution of Simufact engineering GmbH (Kzso and Khazan) is funded through the BMBF-project 03ZZ0210J “Zwanzig20 – Additiv-Generative Fertigung – Verbundvorhaben: ImProVe; TP10: Entwicklung Simulationstool“ by the German Federal Ministry of Education and Research.

Furthermore the authors would like to thank Hydro Aluminium Rolled Products GmbH who provided the material for specimens used in this investigation.

### REFERENCES

- [1] D. S. GNANAMUTHU: *Cladding, US Patent 3,952,180, 1976*
- [2] J. MAZUMDER, D. DUTTA, N. KIKUCHI, A. GOSH: 'Closed loop direct metal deposition: art to part', *Optics and Lasers in Engineering*, Vol. 34, pp. 397-414, 2000
- [3] P. KHAZAN and R. RAJPUT: 'Experimental and numerical investigations of reconditioning of ship engine components by laser cladding', *Proc. of the 4<sup>th</sup> International Workshop on Thermal Forming and Welding Distortions*, Eds.: F. Vollertsen, H. Tetzl, BIAS Verlag, Bremen, pp. 1-12, 2014.
- [4] G. BRANNER: 'Modellierung transienter Effekte in der Struktursimulation von Schichtbauverfahren', *Dissertation*, TU München, 2010
- [5] F. BRÜCKNER, D. LEPSKI, E. BEYER: 'Modelling the Influence of Process Parameters and Additional Heat Sources on Residual Stresses in Laser Cladding', *Journal of Thermal Spray Technology*, Vol. 16, No. 3, pp. 355-373, 2006
- [6] P. V. RF RIVINDAR REDDY, G. CHANDRA MOHAN REDDY, P. RADHAKRISHNAE PRASAD: 'A Review on Finite Element Simulations in Metal Forming', *International Journal of Modern Engineering Research*, Vol. 2, Issue 4, pp. 2326-2330, 2012
- [7] I. NEUBAUER: 'Verschweißen eines Umformteils mit einem additiv gefertigten Bauteil unter Berücksichtigung der Fertigungshistorie', *19th Simufact Round Table*, Marburg, 2018.
- [8] N. J. REDDY, K. D. GARTLING: 'The finite element method in heat transfer and fluid dynamics', CRC Press, 2001.
- [9] P. HAUPT: 'Continuum Mecanics and Theory of Materials', Springer, 2002
- [10] J. ALTENBACH and S. A. SACHAROV: 'Die Methode der finiten Elemente in der Festkörpermechanik', Hanser, 1982
- [11] H. PARISCH: 'Festkörper-Kontinuumsmechanik', Teubner, 2003